Received: 20 April 2020 | Revised: 26 July 2020 | Accepted: 10 September 2020
DOI: 10.1002/aoc.6119

FULL PAPER

Applied Organometallic Chemistry WILEY

# Synthesis, characterization, and application of $CoFe_2O_4$@amino-2-naphthol-4-sulfonic acid as a novel and reusable catalyst for the synthesis of spirochromene derivatives

**Homayoun Faroughi Niya** | **Nourallah Hazeri** | **Maryam Fatahpour**

Department of Chemistry, Faculty of Science, University of Sistan and Baluchestan, Zahedan, Iran

**Correspondence**
Nourallah Hazeri, Department of Chemistry, Faculty of Science, University of Sistan and Baluchestan, P.O. Box 98135-674, Zahedan, Iran.
Email: nhazeri@chem.usb.ac.ir; n_hazeri@yahoo.com

**Funding information**
Research Council of University of Sistan and Baluchestan

In the present work, 1-amino-2-naphthol-4-sulfonic acid immobilized on functionalized $CoFe_2O_4$ nanoparticles was successfully synthesized as a new, efficient, and recoverable catalyst and tested for the synthesis of spirochromene derivatives by a simple, green, and inexpensive procedure. This magnetically heterogeneous nanocatalyst was characterized by various techniques such as Fourier transform infrared (FT-IR), thermal gravimetric analysis (TGA)/derivative thermogravimetric (DTG), X-ray diffraction (XRD), MAP, transmission electron microscopy (TEM), energy-dispersive X-ray spectroscopy (EDS), vibrating sample magnetometer (VSM), Brunauer–Emmett–Teller (BET), and scanning electron microscopy (SEM) analyses. The novel synthesized nanocatalyst can be easily separated and can also be reused several times without appreciable loss in its catalytic activity. Furthermore, in comparison with previous reports, this nanocatalyst showed high thermal stability and acidic properties.

**KEYWORDS**
1-Amino-2-naphthol-4-sulfonic acid, ANSA-$CoFe_2O_4$, magnetic nanocatalyst, recoverable nanocatalyst, spirochromene derivatives

## 1 | INTRODUCTION

In recent years, nanomaterials have drawn considerable interest due to their diverse applications in material science, medical, biology, and chemistry.[1,2] These materials, also, have been applied broadly in the fields of environmental remediation as nanoadsorbents for their high reactivity, negligible internal diffusion resistance, and high surface to volume ratio properties.[3,4] Magnetic nanoparticles (MNPs) are one of the important groups of nanomaterials that demonstrated individual properties such as inhibition of centrifugation procedures and the inevitable loss of solid catalysts in the separation process. These materials have been extensively studied as inorganic supports in the synthesis of semi heterogeneous catalysts.[5–7] Also, MNPs are a bridge between homogeneous and heterogeneous catalysis for their surface functionalization.[8–10] Furthermore, the utilization of MNPs in catalysis systems was increased. Superior characteristics of MNPs such as high magnetic properties lead to its easy collection from the reaction mixture, high surface area to volume ratio, and most importantly, eco-friendly and nontoxic procedure.[11] Some MNPs that used in catalytic applications include iron oxide ($Fe_3O_4$), cobalt ferrite ($Fe_2CoO_4$), maghemite ($\gamma$-$Fe_2O_3$), and zinc ferrite ($ZnFe_2O_4$).[12–15] Today, great attention has been paid to cobalt ferrite ($CoFe_2O_4$) nanocrystals with spinel structure due to their superior characteristics, such as high saturation magnetization, large surface area-to-volume ratio, and shape-dependent magnetic behavior.[16–22] As a review of previous studies, many functionalized $CoFe_2O_4$ MNPs have been reported as a heterogeneous catalyst in multicomponent reactions (MCRs) such as $CoFe_2O_4@SiO_2@CPTMS$,[13] $CoFe_2O_4@SiO_2\text{-}SO_3H$,[23] $CoFe_2O_4@SiO_2\text{-}PTA$,[24] $CoFe_2O_4/TMU\text{-}17\text{-}NH_2$,[25] $CoFe_2O_4$@l-asparagine-Cu/Ni,[26] $CoFe_2O_4$@glycine-M,[27] $CoFe_2O_4$@Pr.[28]

Spiro heterocycles play a superior role in modern organic chemistry. Synthesis of new spiro heterocycles has been widely reported such as spiro[chromene-4,3′-indoles], spiro[indole-3,4′-quinolines], and spiropyranopyrazoles.[29–31] Among various spiro heterocycles, chromene-containing spirooxindoles have attracted significant attention because of their remarkable biological properties including antianaphylactic, anticancer, anticoagulant, diuretic, and spasmolitic activities. These compounds usually were synthesized through a three-component reaction of acenaphthoquinone or isatin with cyanoacetic ester or malononitrile and 1,3-dicarbonyl compounds.[32–35]

In continuation of the development of the synthesis of $CoFe_2O_4$ MNPs as a green catalyst in MCRs, herein, 1-amino-2-naphthol-4-sulfonic acid (ANSA) has been successfully immobilized onto $CoFe_2O_4$ nanostructured and further used as a novel efficient and reusable nanocatalyst with excellent catalytic activity for the synthesis of spirochromene derivatives via the reaction of one equivalent of 1,2-diketones and malononitrile with one equivalent of different CH-activated compounds (Scheme 1).

# 2 | EXPERIMENTAL

## 2.1 | General

Melting points and infrared (IR) spectra of all compounds were determined using an Electro thermal 9100 apparatus and a Fourier transform infrared (FT-IR)-JASCO-460 plus spectrometer. The $^1H$ and $^{13}C$ nuclear magnetic resonance (NMR) spectra of known compounds were recorded on a Bruker DRX-300 Avance instrument in 300 MHz for $^1H$ NMR using dimethyl sulfoxide (DMSO) as a solvent. All reagents and solvents were obtained from Aldrich and Merck and were used without further purification. Field emission scanning electron microscope (FESEM) and transmission electron microscopy (TEM) images of the synthesized nanoparticles were obtained by a MIRA3 TESCAN-XMU scanning electron microscope and a Leo 912 AB transmission electron microscope, respectively. The magnetic properties of the synthesis nanoparticles were studied by vibrating sample magnetometer (VSM) of Lake Shore Cryotronics Company. The thermal behavior of the synthesis nanoparticles was studied by a TG 209F3 NETZSCH thermo-gravimetric analysis.

## 2.2 | Synthesis of the magnetic $CoFe_2O_4$ nanoparticles

A total of 2.0 mmol of $FeCl_3.6H_2O$ and 1.0 mmol of $CoCl_2.6H_2O$ were dissolved in 100 ml of distilled water under nitrogen flow. Then, a KOH solution (1 M) was slowly added to the salt solution dropwise under vigorous stirring at 1000 rpm. After reaching the pH to 11–12, the mixture was refluxed for 3 h at 140°C. Finally, the synthesized $CoFe_2O_4$

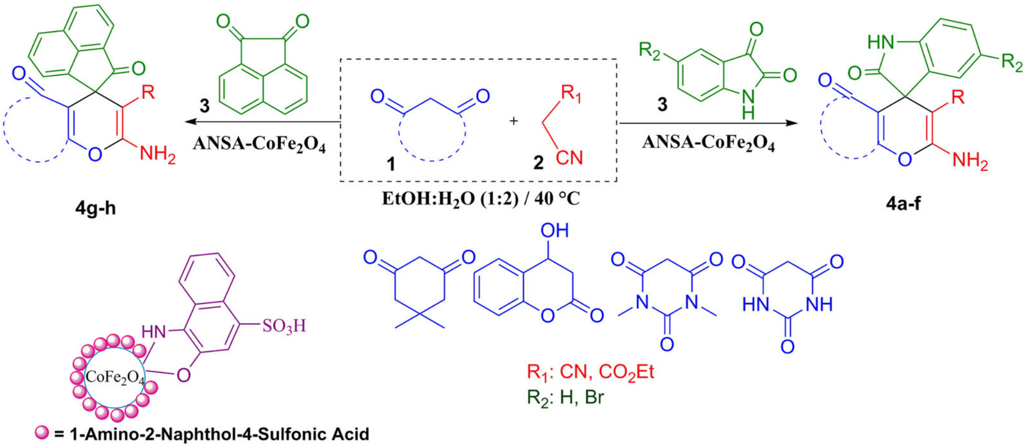

**SCHEME 1** Synthesis of spirochromene in the presence of ANSA-CoFe2O4 as a magnetic nanocatalyst

nanoparticles (black precipitate) were separated by an external magnet and washed several times with water and ethanol and dried for 3 h at 60°C in an oven.

### 2.3 | Synthesis of magnetite nanoparticles coated by 1-amino-2-naphthol-4-sulfonic acid

An appropriate amount of synthesized $CoFe_2O_4$ nanoparticles (0.2 g) was ultrasonically dispersed in 20 ml of ethanol (96%) for 20 min. Then, to this suspension, 0.4 g of 1-amino-2-naphthol-4-sulfonic acid was added. The reaction mixture was refluxed for 24 h at 100°C under $N_2$ atmosphere. Finally, the achieved ANSA-$CoFe_2O_4$ nanoparticles were separated by an external magnet and washed several times with water, ethanol, and acetonitrile to remove unreacted material and dried at 60°C.

### 2.4 | General procedure for three-component synthesis of spirochromene derivatives

A mixture of CH-acid (1.0 mmol), ethyl cyanoacetate or malononitrile (1.0 mmol), acenaphthoquinone or isatin derivatives (1.0 mmol), and ANSA-$CoFe_2O_4$ (10 mg) in $H_2O$:EtOH (2:1) (6 ml) was magnetically stirred at 40°C in an oil bath, and the reaction was monitored by thin-layer chromatography (TLC). After completion of the reaction, the product was dissolved in hot ethanol and DMSO, and the ANSA-$CoFe_2O_4$ nanocatalyst was conveniently removed from the solution by an external magnet. Finally, the resulting solution was cooled to room temperature and the crude product was crystallized to afford the pure products. The pure products were identified by IR, MP, and $^1$H-NMR. The spectra of selected compounds have been reported in the Supporting Information.

### 2.5 | Selected spectra for seven known products are given below

#### 2.5.1 | 2-amino-7,7-dimethyl-2′,5-dioxo-5,6,7,8-tetrahydrospiro[chromene-4,3′-indoline]-3-carbonitrile (4a)

mp: 289–292°C [36]. IR (KBr): $\nu_{max}$ 3377, 3314, 3141, 2959, 2190, 1723, 1682, 1293 $cm^{-1}$; $^1$H NMR (DMSO-d6, 300 MHz) δ = 1.03 (s, 6H, $2CH_3$), 2.15 (s, 2H, $CH_2$), 2.57 (s, 2H, $CH_2$), 6.81–7.24 (m, 6H, Ar-H, and $NH_2$), 10.42 (s, 1H, NH) ppm.

#### 2.5.2 | 2′-amino-2,5′-dioxo-5′H-spiro[indoline-3,4′-pyrano[3,2-*c*]chromene]-3′-carbonitrile (4b)

mp: 288–290°C [36]. IR (KBr): $\nu_{max}$ 3295, 3196, 2205, 1711, 1673 $cm^{-1}$; $^1$H NMR (DMSO-d6, 300 MHz) δ = 7.49–8.35 (m, 10H, Ar-H, and $NH_2$), 8.37 (s, 1H, NH) ppm.

#### 2.5.3 | 7′-amino-2,2′,4′-trioxo-1′,2′,3′,4′-tetrahydrospiro[indoline-3,5′-pyrano[2,3-*d*]pyrimidine]-6′-carbonitrile (4c)

mp: 270–273°C [36]. IR (KBr): $\nu_{max}$ 3354, 3305, 3142, 2955, 2203, 1721, 1673, 1617, 1112; $^1$H NMR (DMSO-d6, 300 MHz): δ = 6.82 (d, 1H, $J = 7.5$ Hz, ArH), 6.94 (t, 1H, $J = 7.5$ Hz, ArH), 7.15–7.21 (m, 2H, ArH), 7.39 (s, 2H, $NH_2$), 10.51 (s, 1H, NH), 11.16 (s, 1H, NH), 12.33 (s, 1H, NH) ppm.

#### 2.5.4 | 7′-amino-1′,3′-dimethyl-2,2′,4′-trioxo-1′,2′,3′,4′-tetrahydrospiro[indoline-3,5′-pyrano[2,3-*d*]pyrimidine]-6′-carbonitrile (4d)

mp: 215–218°C [36]. $^1$H NMR (DMSO-d6, 300 MHz): δ = 3.04 (s, 3H, $CH_3$), 3.41 (s, 3H, $CH_3$), 6.84 (d, 1H, $J = 7.8$ Hz, ArH), 6.93 (td, 1H, $J = 7.2$ Hz, $J = 0.6$ Hz, ArH), 7.13–7.22 (m, 2H, ArH), 7.59 (s, 2H, $NH_2$),10.53 (s, 1H, NH) ppm.

#### 2.5.5 | Ethyl7′-amino-5-bromo-1′,3′-dimethyl-2,2′,4′-trioxo-1′,2′,3′,4′-tetrahydrospiro[indoline-3,5′-pyrano[2,3-*d*]pyrimidine]-6′-carboxylate (4e)

mp: 227–228°C [36]. $^1$H NMR (DMSO-d6, 300 MHz): δ = 0.87 (t, 3H, $J = 7.2$ Hz, $CH_3$), 3.04 (s, 3H, $CH_3$), 3.42 (s, 3H, $CH_3$), 3.46 (q, 2H, $J = 7.2$ Hz, $OCH_2$), 6.68 (d, 1H, $J = 8.1$ Hz, ArH), 7.20 (1H, d, $J = 1.8$ Hz, ArH), 7.26 (dd, $J = 8.1$ Hz, $J = 2.1$ Hz, 1H, ArH), 8.13 (s, 2H, $NH_2$),10.42 (s, 1H, NH) ppm.

#### 2.5.6 | 2′-amino-7′,7′-dimethyl-2,5′-dioxo-5′,6′,7′,8′-tetrahydro-2*H*-spiro[acenaphthylene-1,4′-chromene]-3′-carbonitrile (4g)

mp: 269–270°C [36]. $^1$H NMR (DMSO-d6, 300 MHz): 1.03 (s, 6H, $2CH_3$), 2.09 (dd, 2H, $J = 16.02$ Hz, $J = 12.03$ Hz,

$CH_2$), 2.64 (dd, 2H, *J* = 19.35 Hz, *J* = 13.5 Hz, $CH_2$), 7.32–8.28 (m, 8H, ArH, and $NH_2$) ppm.

### 2.5.7 | 2′-amino-2,5′-dioxo-2H,5′H-spiro[acenaphthylene-1,4′-pyrano[3,2-*c*]chromene]-3′-carbonitrile (4h)

mp: 288–291°C [36]. $^1$H NMR (DMSO-d6, 300 MHz): 7.50 (d, 1H, *J* = 8.1 Hz, ArH), 7.57 (t, 1H, *J* = 7.5 Hz, ArH), 7.64–7.81 (m, 5H, ArH, $NH_2$), 7.89 (t, 1H, *J* = 7.8 Hz, ArH), 7.99–8.07 (m, 3H, ArH), 8.36 (d, 1H, *J* = 7.8 Hz, ArH) ppm.

## 3 | RESULTS AND DISCUSSION

### 3.1 | Catalyst characterizations

In this study, an applied strategy for the synthesis of the 1-amino-2-naphthol-4-sulfonic acid supported on $CoFe_2O_4$ MNPs was described (Scheme 2). Then, the synthesized $CoFe_2O_4$@ANSA nanocatalyst was characterized by scanning electron microscopy (SEM), X-ray mapping, energy-dispersive X-ray spectroscopy (EDS), FT-IR, differential thermal analysis (DTA), thermal gravimetric analysis (TGA), X-ray diffraction (XRD), Brunauer–Emmett–Teller (BET), and VSM techniques.

To confirm the immobilization of 1-amino-2-naphthol-4-sulfonic acid on the surface of $CoFe_2O_4$ MNPs, FT-IR spectroscopy was initially applied. Figure 1 shows the FT-IR spectra of $CoFe_2O_4$ (a), ANSA-$CoFe_2O_4$ (b) nanoparticles. As can be seen, the band at 618 cm$^{-1}$ is assigned to Fe—O and Co—O bonds in $CoFe_2O_4$ (Figure 1a) which shifts to 595 cm$^{-1}$ after coating with ANSA (Figure 1b). The broad band at 3373 cm$^{-1}$ is attributed to adsorbed water molecules and the Co—OH stretching vibration. The bands at 1046–1200 cm$^{-1}$ are assigned to the stretching mode of the S—O and S═O bands of —$SO_3H$ groups on the ANSA-$CoFe_2O_4$ surface.

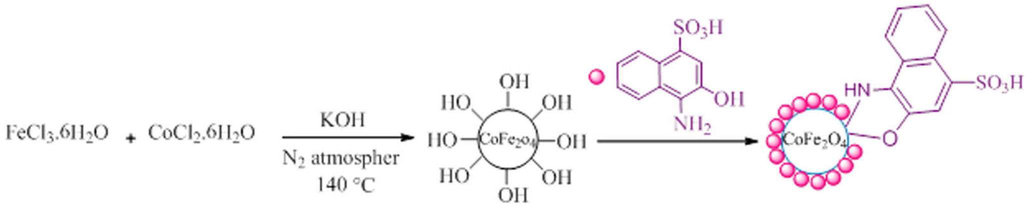

SCHEME 2 Preparation of ANSA-CoFe2O4

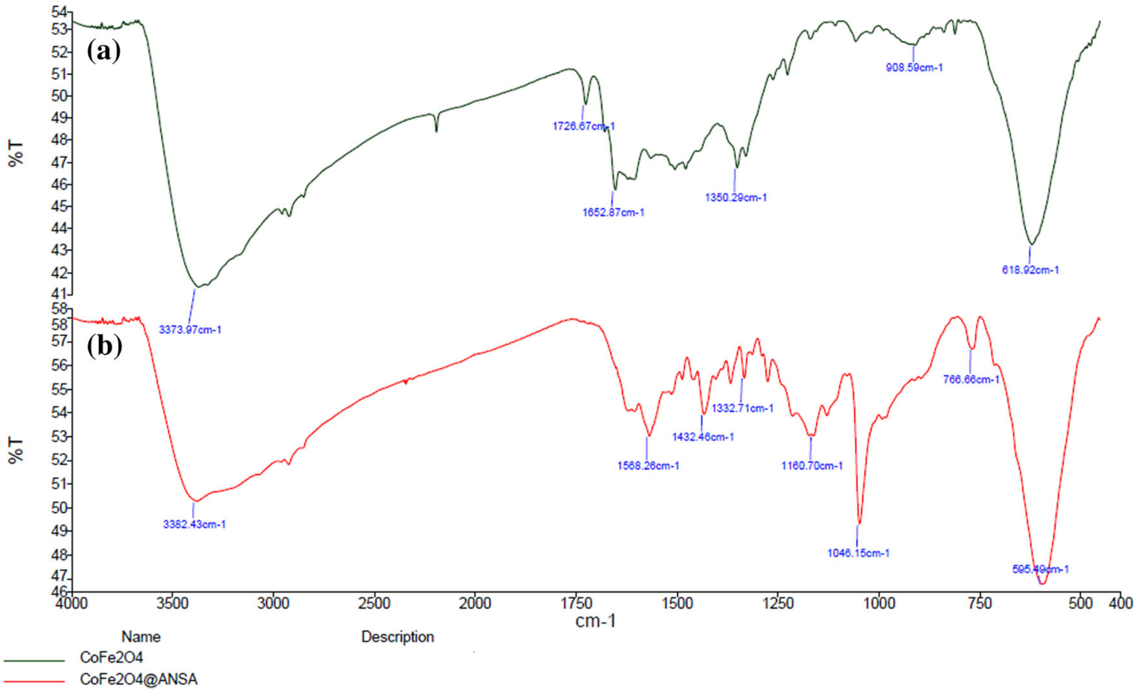

FIGURE 1 Fourier transform infrared (FT-IR) spectra of $CoFe_2O_4$ (a) and $CoFe_2O_4$@ANSA (b) magnetic nanoparticles (MNPs)

FESEM images of $CoFe_2O_4$ and ANSA-$CoFe_2O_4$ nanoparticles are shown in Figure 2. As can be seen, a significant change in the surface morphology of $CoFe_2O_4$ MNPs occurs after coting 1-amino-2-naphthol-4-sulfonic acid. Also, the size distribution and the surface morphology of $CoFe_2O_4$ MNPs (**3a**) and ANSA-$CoFe_2O_4$ (**3b**) are different. The $CoFe_2O_4$ and ANSA-$CoFe_2O_4$ nanoparticles have an average size of approximately 19.46 and 27.94 nm, respectively. (Figure 3a,b). This change in size is due to the immobilization of ANSA on the surface of $CoFe_2O_4$ MNPs.

The distribution of elements in $CoFe_2O_4$ and ANSA-$CoFe_2O_4$ nanoparticles was investigated by EDS analysis (Figure 4a,b). As can be seen, the presence of nitrogen (N, 3.96%), carbon (C, 28.00%), and sulfur (S, 3.68%) elements confirm the successful synthesis of ANSA-$CoFe_2O_4$ (Figure 4b). Also, Figure 5 illustrates the X-ray mapping of ANSA-$CoFe_2O_4$ nanoparticles. As can be seen, the homogenous presence of 1-amino-2-naphthol-4-sulfonic acid on the surface of $CoFe_2O_4$ MNPs was confirmed.

TEM images were used to investigate the nanostructure morphology of ANSA-$CoFe_2O_4$. As shown in Figure 6, TEM images of ANSA-$CoFe_2O_4$ nanoparticles displayed a cubic shape with an average size about 17.42 nm (Figure 7) that confirmed FESEM results. Furthermore, ANSA-$CoFe_2O_4$ nanoparticles were identified as a core-shell structure.

To study the thermal behavior of ANSA-$CoFe_2O_4$ nanoparticles, TGA analysis was applied. As shown in Figure 8, the TGA curve of ANSA-$CoFe_2O_4$ shows three weight-loss steps. A small weight loss (3.84%) between 0°C and 280°C is attributed to the desorption of adsorbed solvents and materials. A second, larger weight loss between 280 and 380°C could be attributed to the immobilized sulfuric acid groups ($SO_3H$). The organic residue on the surface of ANSA-$CoFe_2O_4$ nanoparticles was decomposed between 380°C and 500°C. In accordance with the TGA curve (total mass loss of 16.99%), 169.9 mg of ANSA was loaded on 1 g of $CoFe_2O_4$ nanoparticles. And the further weight loss at above 500°C can be attributed to the change of catalyst

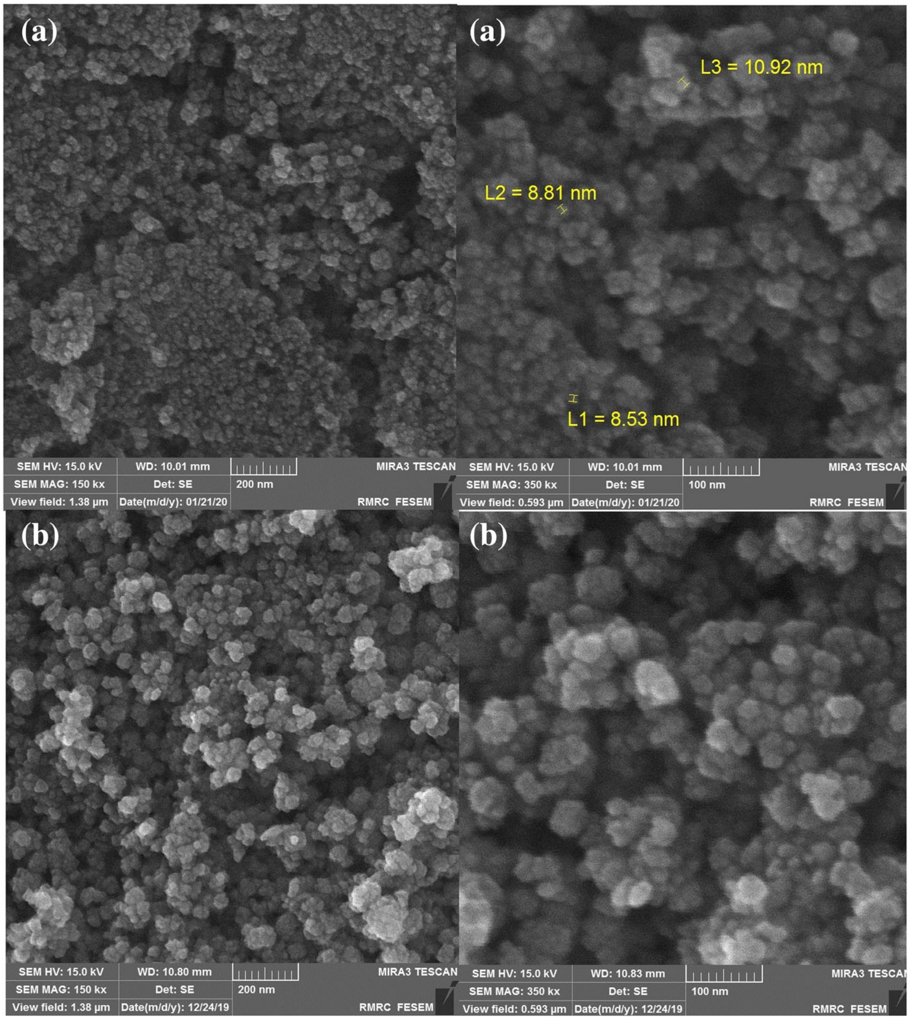

**FIGURE 2** Field emission scanning electron microscope (FESEM) images of $CoFe_2O_4$ (a) and $CoFe_2O_4$@ANSA (b) magnetic nanoparticles (MNPs)

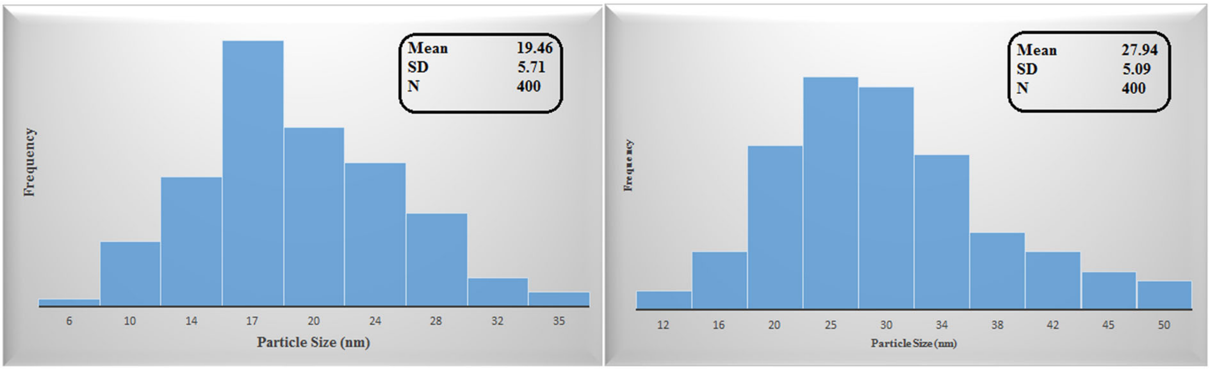

**FIGURE 3** The size histogram of $CoFe_2O_4$ (a) and $CoFe_2O_4$@ANSA (b) magnetic nanoparticles (MNPs)

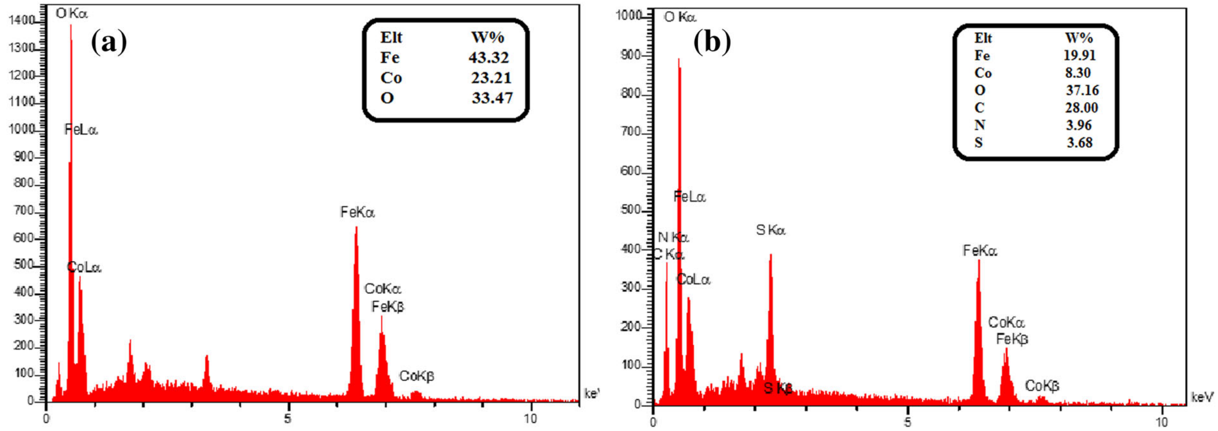

**FIGURE 4** Energy-dispersive X-ray spectroscopy (EDS) spectrum of $CoFe_2O_4$ (a) and $CoFe_2O_4$@ANSA (b) magnetic nanoparticles (MNPs)

structure. TGA analysis results confirmed the immobilization of ANSA on the surface of $CoFe_2O_4$ MNPs. Also, the DTG curve indicated that ANSA-$CoFe_2O_4$ nanoparticles are stable below 337°C.

The XRD patterns of $CoFe_2O_4$ (curve **a**) and ANSA-$CoFe_2O_4$ nanoparticles (curve **b**) are illustrated in Figure 9. According to JCPDS card no. 03–0864, The XRD diffraction pattern of $CoFe_2O_4$ displays seven diffraction peaks at 18.24°, 30.06°, 35.45°, 43.47°, 53.88°, 57.17°, and 62.73°, which are assigned to (1 1 1), (2 2 0), (3 1 1), (4 0 0), (4 2 2), (5 1 1), (4 4 0) crystallographic faces of magnetite. In the XRD pattern of ANSA-$CoFe_2O_4$ (Figure 9b), the reflection of the amorphous organic layer (ANSA) could be seen at $2\theta = 0°–20°$ as a broad band, that confirmed the immobilization of ANSA on the surface of $CoFe_2O_4$ MNPs.

The magnetic property of $CoFe_2O_4$ and ANSA-$CoFe_2O_4$ nanoparticles was investigated using room-temperature VSM analysis. As shown in Figure 10, the magnetic saturation (Ms) values of $CoFe_2O_4$ and ANSA-$CoFe_2O_4$ are about 28.41, 29.45 emu $g^{-1}$, respectively. No significant change in the Ms values of ANSA-$CoFe_2O_4$ occurs after the immobilization of ANSA on the surface of $CoFe_2O_4$ MNPs.

The factors of surface area, pore distribution, and pore volume of ANSA-$CoFe_2O_4$ MNPs have been determined by the BET analysis. Nitrogen adsorption/desorption isotherm, BET plot, and Barrett, Joyner, and Halenda (BJH) pore size distribution for ANSA-$CoFe_2O_4$ MNPs are shown in Figure 11a–c. According to $N_2$ adsorption/desorption, the pore volume of ANSA-$CoFe_2O_4$ MNPs is 0.659 $cm^3$ $g^{-1}$. The BJH and BET analyses displayed that the average pore diameter and the available surface area for ANSA-$CoFe_2O_4$ MNPs are 1.85 nm and 2.87 $m^2$ $g^{-1}$, respectively. As regards the average pore diameter is less than 2 nm, so the ANSA-$CoFe_2O_4$ nanocatalyst is microporous.

## 3.2 | Catalytic study

To demonstrate the catalytic activity of ANSA-$CoFe_2O_4$ nanoparticles, the synthesis of spirochromene derivatives was investigated in the presence of

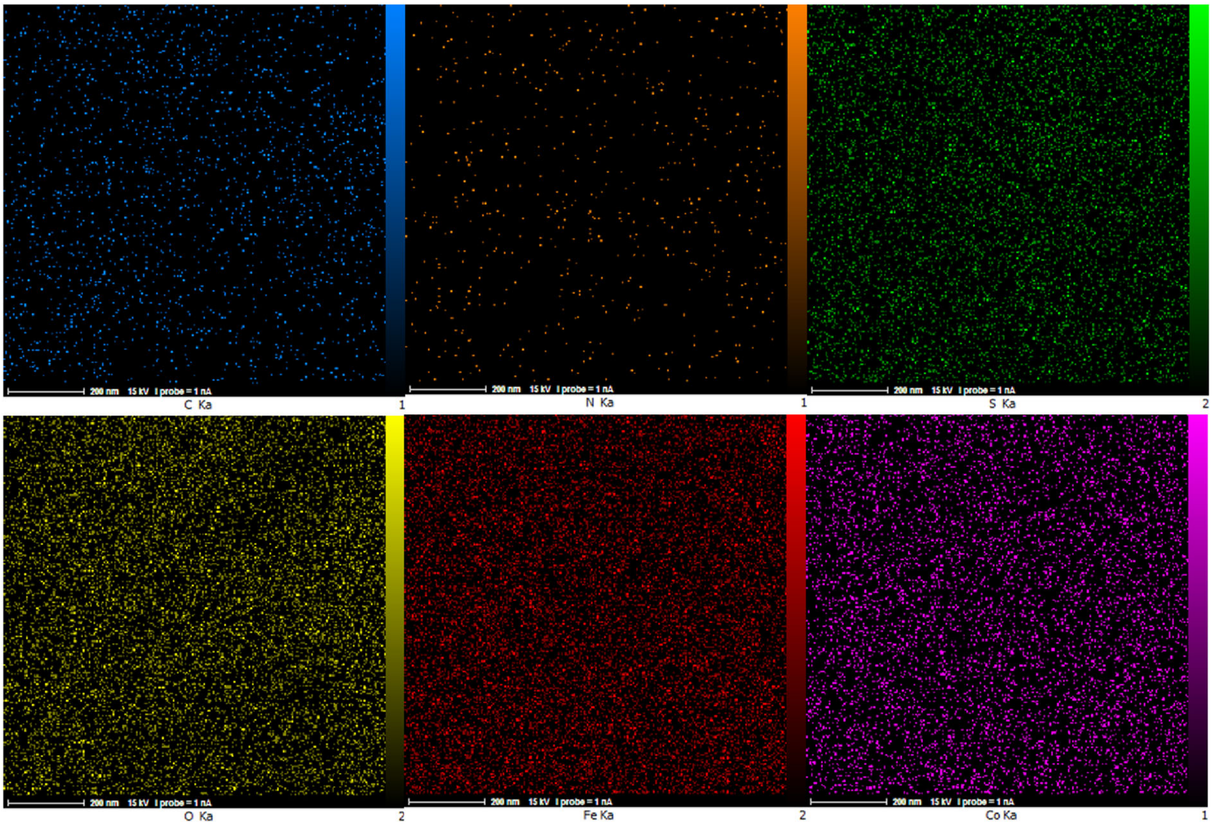

**FIGURE 5** The X-ray mapping of $CoFe_2O_4$@ANSA magnetic nanoparticles (MNPs)

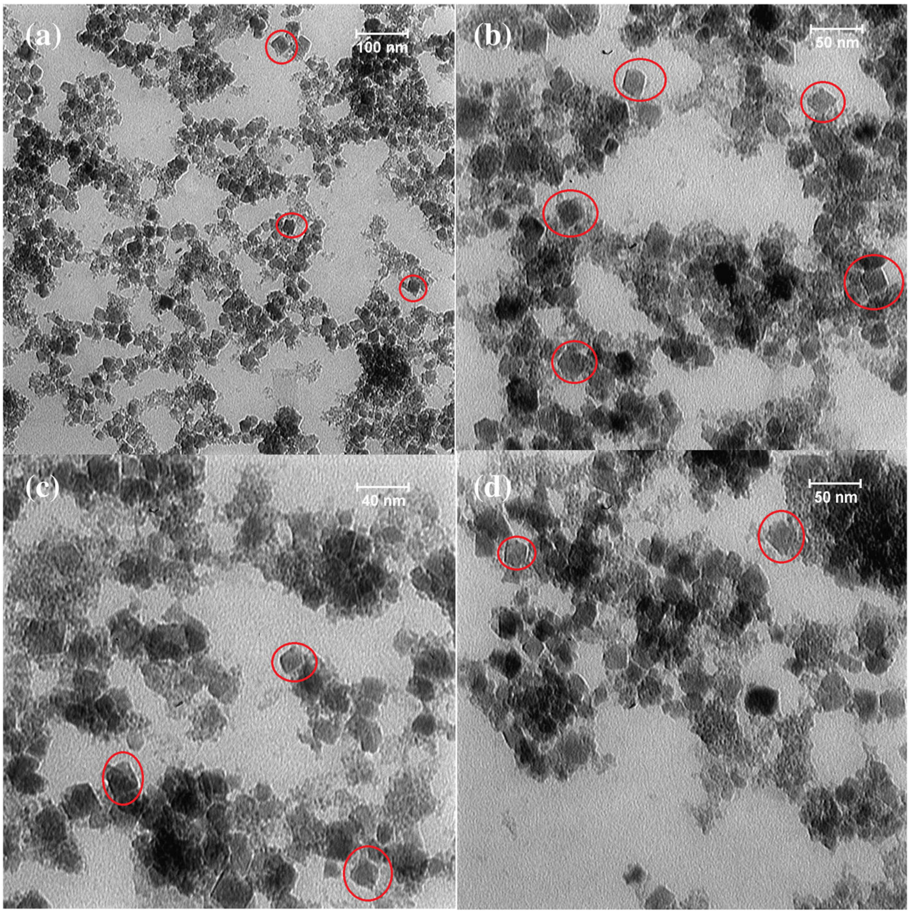

**FIGURE 6** Transmission electron microscopy (TEM) images of $CoFe_2O_4$@ANSA magnetic nanoparticles (MNPs)

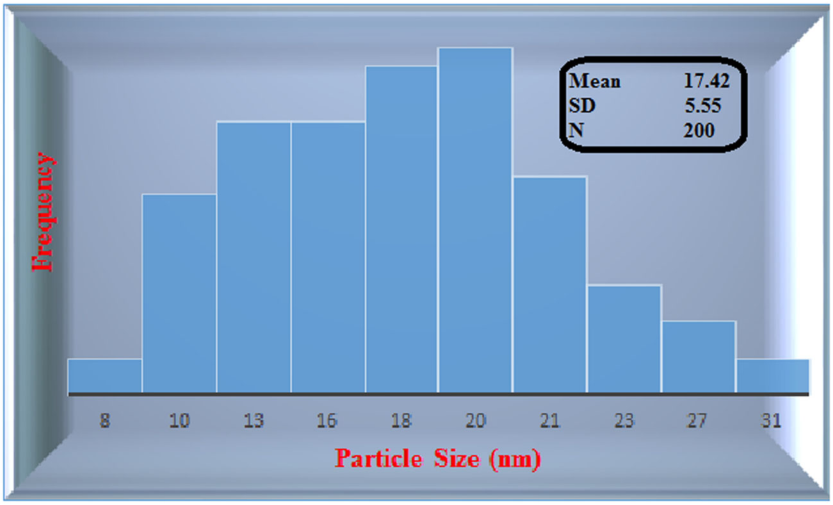

**FIGURE 7** The size histogram of $CoFe_2O_4$@ANSA magnetic nanoparticles (MNPs)

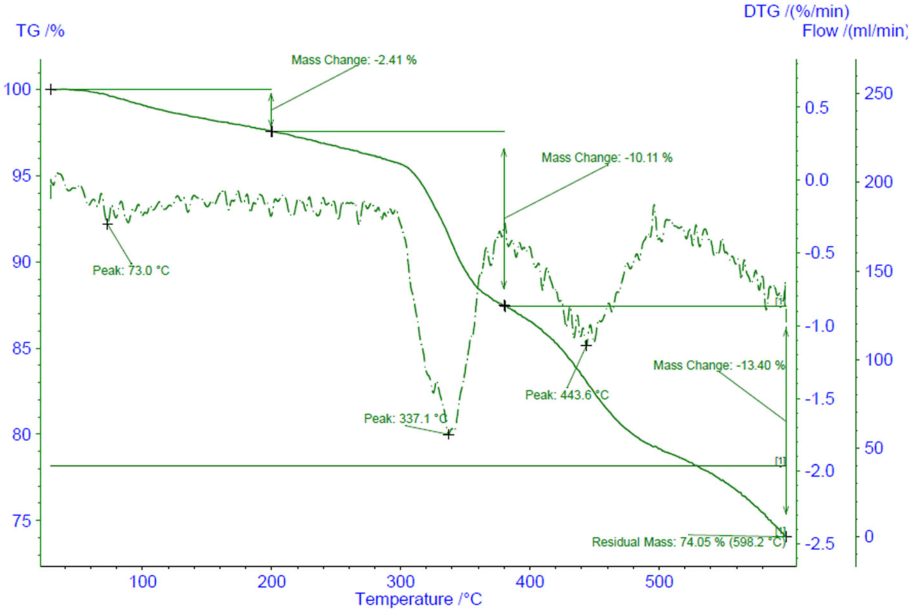

**FIGURE 8** Thermal gravimetric analysis (TGA) and derivative thermogravimetric (DTG) curves of $CoFe_2O_4$@ANSA magnetic nanoparticles (MNPs)

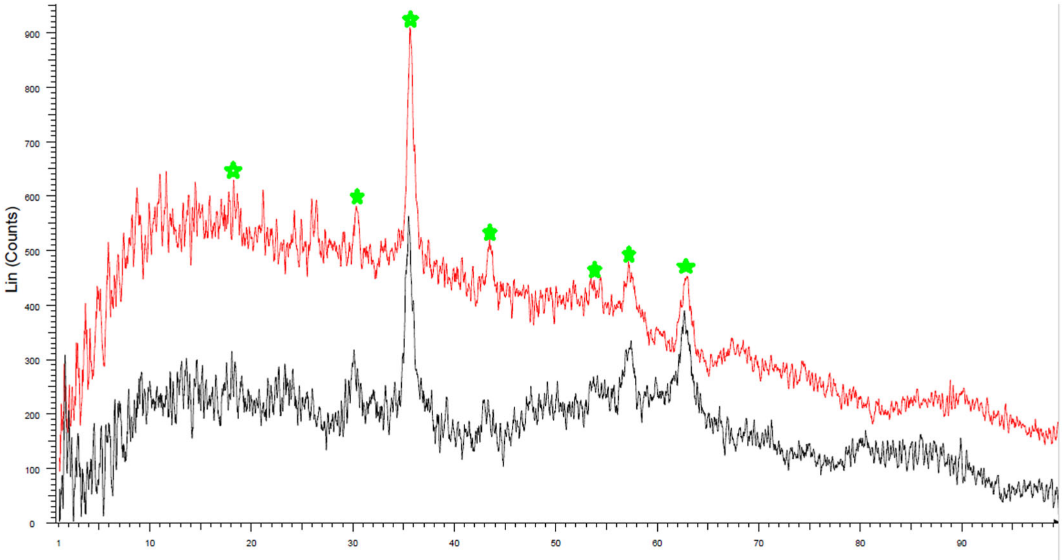

**FIGURE 9** X-ray diffraction (XRD) pattern of $CoFe_2O_4$ (a) and $CoFe_2O_4$@ANSA (b) magnetic nanoparticles (MNPs)

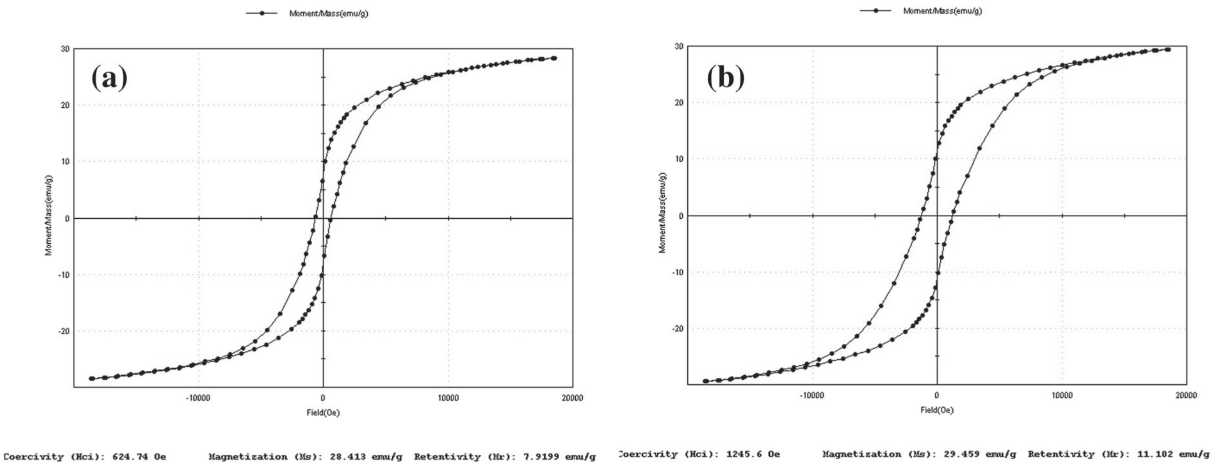

**FIGURE 10** Vibrating sample magnetometer (VSM) spectra of $CoFe_2O_4$ (a) and $CoFe_2O_4$@ANSA (b) magnetic nanoparticles (MNPs)

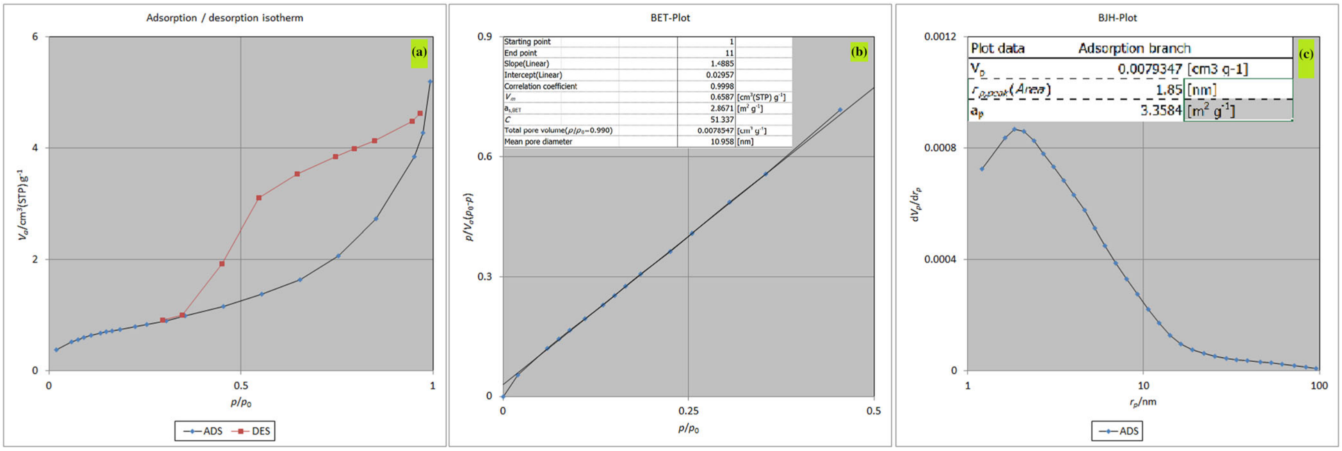

| | | |
|---|---|---|
| Starting point | 1 | |
| End point | 11 | |
| Slope(Linear) | 1.4885 | |
| Intercept(Linear) | 0.02957 | |
| Correlation coefficient | 0.9998 | |
| $V_m$ | 0.6587 | [$cm^3$(STP) $g^{-1}$] |
| $a_{s,BET}$ | 2.8671 | [$m^2$ $g^{-1}$] |
| $C$ | 51.337 | |
| Total pore volume($p/p_0$=0.990) | 0.0078547 | [$cm^3$ $g^{-1}$] |
| Mean pore diameter | 10.958 | [nm] |

| Plot data | Adsorption branch | |
|---|---|---|
| $V_p$ | 0.0079347 | [cm3 g-1] |
| $r_{p,peak}$(Area) | 1.85 | [nm] |
| $a_p$ | 3.3584 | [$m^2$ $g^{-1}$] |

**FIGURE 11** Nitrogen adsorption/desorption isotherm (a), Brunauer–Emmett–Teller (BET) plot (b), and BJH pore size distribution (c) of the ANSA-$CoFe_2O_4$ nanocatalyst

ANSA-$CoFe_2O_4$ nanoparticles. For achieving this purpose, the reaction conditions (solvent, amount of catalyst, and temperature) were first optimized and the reaction between isatin, dimedone, and malononitrile was chosen as a model reaction. Initially, the model reaction carried out in different solvents in the presence of 0.01 g of ANSA-$CoFe_2O_4$ nanocatalyst at 50°C. In these conditions, The best result was obtained in $H_2O$:EtOH (2:1) solvent (6 ml) with 94% yields (Table 1, entry 4). In the next step, in order to find a better condition for the synthesis of spirochromene derivatives, the model reaction was performed in the different amounts of catalyst (Table 1). In the absence of the catalyst, no significant improvement was observed. In the presence of the different amounts of catalyst, the yield and rate of reaction were increased. As shown in Table 1, the high catalytic activity of ANSA-$CoFe_2O_4$ nanoparticles was achieved in the presence of 0.01 g of catalyst. The yield of reaction with 0.02 g of catalyst was decreased, that is probably because of the steric hindrance of the nanocatalyst in the reaction mixture and reduces the impact of starting materials. Finally, the temperature effect was explored, and the best result was found in $H_2O$:EtOH (2:1) in the presence of 0.01 g of ANSA-$CoFe_2O_4$ nanocatalyst at 40°C. In this condition, the corresponding product was obtained in 95% yields (Table 1, entry 9).

According to the optimal reaction conditions, the synthesis of spirochromene derivatives was carried out using a variety of diketones and CH-acid compounds, and the results are summarized in Table 2. The results displayed that the synthesis of spirochromene derivatives went well with a broad range of diketones and CH-acid compounds in good to excellent yields (64%–97%) and short reaction times, which confirmed the high catalytic activity of ANSA-$CoFe_2O_4$ nanoparticles.

**TABLE 1** Optimization of reaction conditions for the synthesis of spirochromenes

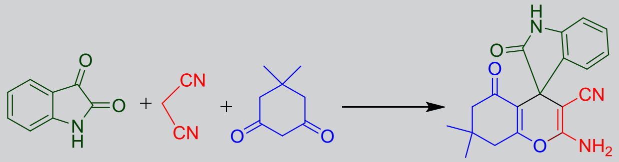

| Entry | Catalyst (g) | Solvent | Temperature (°C) | Time (min) | Yield (%) |
|---|---|---|---|---|---|
| 1 | 0.01 | EtOH | 50 | 5 | 87 |
| 2 | 0.01 | $H_2O$:EtOH (1:1) | 50 | 5 | 89 |
| 3 | 0.01 | $H_2O$ | 50 | 5 | 87 |
| 4 | 0.01 | $H_2O$:EtOH (2:1) | 50 | 5 | 94 |
| 5 | 0.01 | $H_2O$:EtOH (1:2) | 50 | 5 | 90 |
| 7 | 0.005 | $H_2O$:EtOH (2:1) | 50 | 5 | 85 |
| 8 | 0.02 | $H_2O$:EtOH (2:1) | 50 | 5 | 79 |
| **9** | **0.01** | $H_2O$:EtOH (1:2) | **40** | **5** | **95** |
| 10 | 0.01 | $H_2O$:EtOH (1:2) | r.t | 5 | 88 |
| 11 | No catalyst | $H_2O$:EtOH (1:2) | 40 | 15 | 68 |
| 12 | $CoFe_2O_4$ | $H_2O$:EtOH (1:2) | 40 | 10 | 79 |

**TABLE 2** Synthesis of spirochromene derivatives in the presence of ANSA-$CoFe_2O_4$ (0.01 g) in EtOH:$H_2O$ (1:2) at 40°C

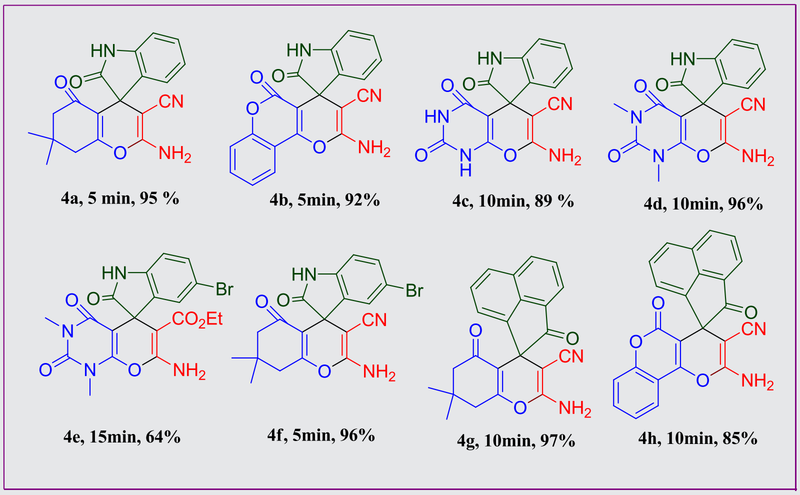

**4a**, 5 min, 95 %

**4b**, 5min, 92%

**4c**, 10min, 89 %

**4d**, 10min, 96%

**4e**, 15min, 64%

**4f**, 5min, 96%

**4g**, 10min, 97%

**4h**, 10min, 85%

According to the proposed mechanism shown in Scheme 3, the ANSA-$CoFe_2O_4$ nanoparticles in the catalytic cycle for the synthesis of spirochromene derivatives act as a Lewis acid catalyst and increase the electrophilicity of the carbonyl group of 1,2-diketones **3**. So immediately, the Knoevenagel condensation of malononitrile **2** (deprotonation by ANSA-$CoFe_2O_4$ MNPs) and 1,2-diketones **3** generates olefin A. Then, intermediate **B** was formed *via* Michael addition of CH-activated compounds **1** and olefin **A**. Finally, intramolecular cyclization and tautomerization happen to give the corresponding products (**4a–h**).

### 3.2.1 | Recyclability study

In order to demonstrate that the ANSA-$CoFe_2O_4$ nanoparticles act as an eco-friendly and green catalyst,

**SCHEME 3** The proposed mechanism for the synthesis of spirochromene in the presence of ANSA-CoFe2O4

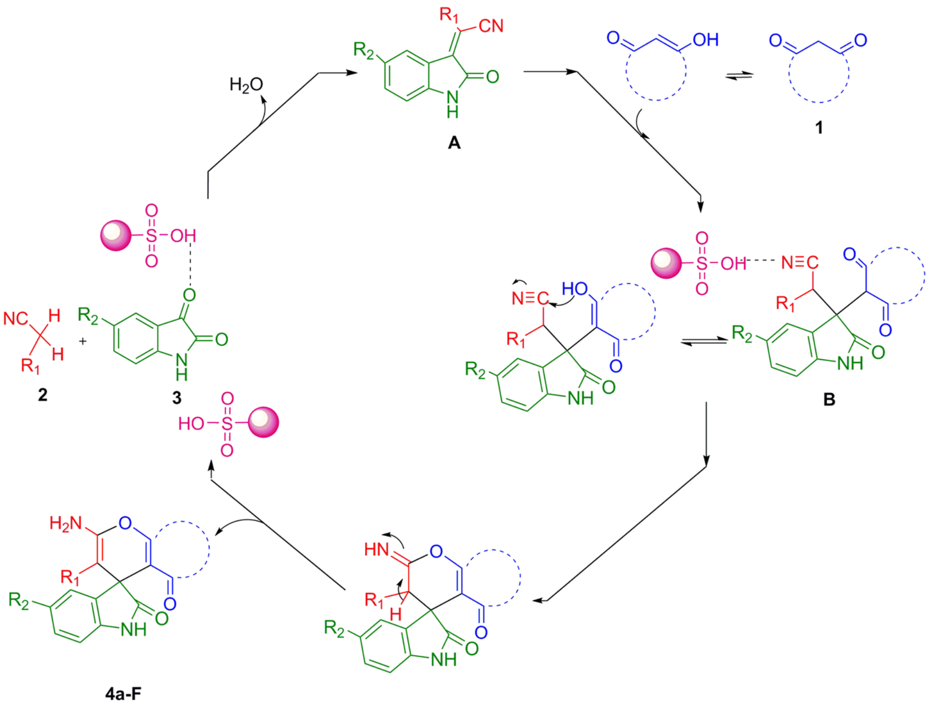

**FIGURE 12** Reusability of $CoFe_2O_4$@ANSA nanocatalyst in the synthesis of 2-amino-7,7-dimethyl-2′,5-dioxo-5,6,7,8-tetrahydrospiro[chromene-4,3′-indoline]-3-carbonitrile

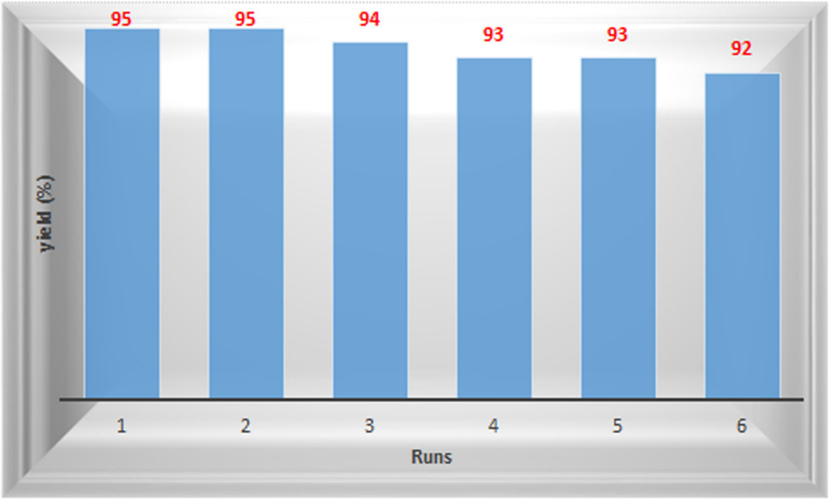

the nanocatalyst must be easily recycled and reused without any significant reduction in its activities. The reaction of isatin with dimedone and malononitrile was chosen as a model reaction to examine the recyclability of the new nanocatalyst. The reaction was performed under the optimal reaction conditions. Upon completion of the reaction, the corresponding product was dissolved in hot ethanol and DMSO, and hen the ANSA-$CoFe_2O_4$ nanocatalyst was conveniently removed from the solution by an external magnet. The ANSA-$CoFe_2O_4$ nanocatalyst was washed by ethanol four to five times to remove any organic residues and then dried at 80°C in an oven and reused in the next reactions. As can see in Figure 12, the ANSA-$CoFe_2O_4$ nanocatalyst was reused for six successive runs without any significant loss of activity.

## 3.3 | Comparison

In order to compare the catalytic activity of the ANSA-$CoFe_2O_4$ nanoparticles with other reported catalysts, the compound **4a** was selected as a model and the results were summarized in Table 3. As can be seen, high yield and good reaction time are some advantages of this procedure that confirm the high catalytic activity of the ANSA-$CoFe_2O_4$ nanoparticles.

**TABLE 3** Comparison of the efficiency of ANSA-$CoFe_2O_4$ nanocatalyst with other reported catalysts in the studied reactions

| Product | Catalyst | Amount of catalyst | Condition | Time (min) | Yield (%) | [Ref.] |
|---|---|---|---|---|---|---|
| 4a | QUIN | 20 mol% | EtOH:$H_2O$ (1:1), 70°C | 7 | 94 | Oudi et al.[36] |
| | $NH_4Cl$ | 20 mol% | Water, 70°C | 10 | 92 | Dabiri et al.[37] |
| | $SnO_2$ NPs | 30 mg | EtOH, r.t. | 8 | 96 | Moradi et al.[38] |
| | $Fe_3O_4$/COS@β-CD-$SO_3H$ | 20 mg | $H_2O$, 50°C | 20 | 98 | Mohammadian and Akhlaghinia[39] |
| | $CoFe_2O_4$@$SiO_2$ | 10 mg | EtOH:$H_2O$ (1:1), 80°C | 5 | 98 | Hemmat et al.[40] |
| | $CoFe_2O_4$@$SiO_2$@$SO_3H$ | 10 mg | EtOH:$H_2O$ (1:1), 80°C | 2 | 98 | Zamani-Ranjbar-Garmroodi et al.[41] |
| | ANSA-$CoFe_2O_4$ | 10 mg | $H_2O$:EtOH (2:1), 40°C | 5 | 95 | [This work] |

## 3.4 | Conclusions

In summary, a novel magnetic nanocatalyst, ANSA-$CoFe_2O_4$, has been successfully fabricated *via* a green and simple procedure. The analyses showed that the catalyst has the nanometric size and highly thermally stable. The spherical morphology of $CoFe_2O_4$ was changed to a cubic shape after coating with ANSA. This change caused that the magnetic property of $CoFe_2O_4$ was not decreased by the nonmagnetic layer of ANSA anchored to the surface of the $CoFe_2O_4$ MNPs. Then, the ANSA-$CoFe_2O_4$ MNPs were used as a magnetically sustainable acid nanocatalyst for the synthesis of spirochromene derivatives. This nanocatalyst indicated a highly active heterogeneous catalytic system that can be recovered and reused at least six cycles of reaction without a significant loss in its selectivity and activity. Briefly, in comparison with other nanocatalysts reported, the synthesized nanocatalyst has important advantages such as easy synthesis, high stability, reusability, and excellent yields of products along with short reaction time that make this method useful and attractive.

## ACKNOWLEDGEMENTS

The authors gratefully appreciate the financial support from the Research Council of University of Sistan and Baluchestan.

## AUTHOR CONTRIBUTIONS

**Homayoun Faroughi Niya:** Conceptualization; formal analysis; investigation; methodology; project administration; software. **Nourallah Hazeri:** Investigation; project administration; supervision. **Maryam Fatahpour:** Investigation; methodology.

## DATA AVAILABILITY STATEMENT

The data that support the findings of this study are available from the corresponding author upon reasonable request.

## ORCID

*Homayoun Faroughi Niya* https://orcid.org/0000-0002-2220-4288

*Nourallah Hazeri* https://orcid.org/0000-0002-0560-7245

*Maryam Fatahpour* https://orcid.org/0000-0002-6735-1644

## REFERENCES

[1] L. Qin, G. Zeng, C. Lai, D. Huang, C. Zhang, P. Xu, T. Hu, X. Liu, M. Cheng, Y. Liu, L. Hu, Y. Zhou, *Sens. Actuators, B* **2017**, *243*, 946.

[2] L. Qin, G. Zeng, C. Lai, D. Huang, P. Xu, C. Zhang, M. Cheng, X. Liu, S. Liu, B. Li, H. Yi, *Coord. Chem. Rev.* **2018**, *359*, 1.

[3] S. Karimifard, M. R. Alavi Moghaddam, *Desalination Water Treat.* **2016**, *57*, 16643.

[4] R. K. Ibrahim, M. Hayyan, M. A. AlSaadi, A. Hayyan, S. Ibrahim, *Environ. Sci. Pollut. Res.* **2016**, *23*, 13754.

[5] V. Polshettiwar, R. Luque, A. Fihri, H. Zhu, M. Bouhrara, J. M. Basset, *Chem. Rev.* **2011**, *111*, 3036.

[6] S. Shylesh, V. Schünemann, W. R. Thiel, *Angew. Chem., Int. Ed.* **2010**, *49*, 3428.

[7] F. Liu, F. Niu, N. Peng, Y. Su, Y. Yang, *RSC Adv.* **2015**, *5*, 18128.

[8] K. Azizi, N. Esfandiary, M. Karimi, E. Yazdani, A. Heydari, *RSC Adv.* **2016**, *6*, 89313.

[9] K. Azizi, A. Heydari, *RSC Adv.* **2014**, *4*, 8812.

[10] F. Mollazehi, H. R. Shaterian, *Appl. Organomet. Chem.* **2018**, *32*, e4183.

[11] R. Tarasi, A. Ramazani, M. Ghorbanloo, M. Khoobi, H. Aghahosseini, S. W. Joo, A. Shafiee, **2016**, 1–9.

[12] a) H. Faroughi Niya, N. Hazeri, M. T. Maghsoodlou, *Appl. Organomet. Chem.* **2020**, *34*(4), e5472; b) H. Faroughi Niya, N. Hazeri, M. R. Kahkhaie, M. T. Maghsoodlou, *Res. Chem. Intermed.* **2020**, *46*(3), 1685; c) H. Faroughi Niya, N. Hazeri, M. Fatahpour, M. T. Maghsoodlou, *Res. Chem. Intermed.* **2020**, *46* (7), 3651. https://doi.org/10.1007/s11164-020-04166-z

[13] K. Hemmat, M. A. Nasseri, A. Allahresani, *Appl. Organomet. Chem.* **2019**, *33*(7), e4937.

[14] M. Pashaei, E. Mehdipour, M. Azaroon, *Appl. Organomet. Chem.* **2019**, *33*(1), e4622.

[15] L. Ghandi, M. Kazemi Miraki, M. Karimi, I. Radfar, A. Heydari, *Appl. Organomet. Chem.* **2019**, *33*(1), e4616.

[16] Y. Wang, J. Park, B. Sun, H. Ahn, G. X. Wang, *Chem. – Asian J.* **2012**, *7*, 1940.

[17] D. Fritsch, C. Ederer, *Phys. Rev. B* **2012**, *86*, 014406.

[18] R. Comes, H. X. Liu, M. Kholchov, R. Kasica, J. W. Lu, S. A. Wolf, *Nano Lett.* **2012**, *12*, 2367.

[19] R. S. Turtelli, G. V. Duong, W. Nunes, R. Grössinger, M. Knobel, *J. Magn. Magn. Mater.* **2008**, *320*, e339.

[20] B. Q. Liu, Q. F. Li, B. Zhang, Y. L. Cui, H. F. Chen, G. N. Chen, D. P. Tang, *Nanoscale* **2011**, *3*, 2220.

[21] H. X. Wu, G. Liu, X. Wang, J. M. Zhang, Y. Chen, J. L. Shi, H. Yang, H. Hu, S. P. Yang, *Acta Biomater.* **2011**, *7*, 3496.

[22] Y. D. Yang, S. Priya, Y. U. Wang, J. F. Li, D. Viehland, *J. Mater. Chem.* **2009**, *19*, 4998.

[23] S. Mandal, S. Hazra, S. Sarkar, C. Bodhak, A. Pramanik, *Appl. Organomet. Chem.* **2019**, *33*, e4702.

[24] M. Kooti, E. Nasiri, *J. Mol. Catal. A-Chem.* **2015**, *406*, 168.

[25] M. Yadollahi, H. Hamadi, V. Nobakht, *Appl. Organomet. Chem.* **2019**, *33*(1), e4629.

[26] T. Tamoradi, H. Veisi, B. Karmakar, J. Gholami, *Mat. Sci. Eng. C. Mater* **2020**, *107*, 110260.

[27] T. Tamoradi, A. Ghorbani-Choghamarani, M. Ghadermazi, *Solid State Sci.* **2019**, *88*, 81.

[28] T. Tamoradi, S. M. Mousavi, M. Mohammadi, *New J. Chem.* **2020**, *44*, 3012.

[29] S. A. Pogosyan, D. A. Avakimyan, G. M. Stepanyan, *Russ. J. Org. Chem.* **2016**, *52*, 1308.

[30] S. A. Pogosyan, R. V. Paronikyan, G. M. Stepanyan, A. G. Grigoryan, *Khim. Zh. Arm* **2016**, *69*, 518.

[31] M. Fatahpour, F. N. Sadeh, N. Hazeri, M. T. Maghsoodlou, M. Lashkari, *J. Iran. Chem. Soc* **2017**, *14*, 1945.

[32] J. Skommer, D. Wlodkowic, M. Matto, M. Eray, J. Pelkonen, *Leuk. Res.* **2006**, *30*, 322.

[33] N. Yu, J. M. Aramini, M. W. Germann, Z. Huang, *Tetrahedron Lett.* **2000**, *41*, 6993.

[34] L. Bonsignore, G. Loy, D. Secci, A. Calignano, *Eur. J. Med. Chem.* **1993**, *28*, 517.

[35] L. L. Andreani, E. Lapi, *Boll. Chim. Farm.* **1960**, *99*, 583.

[36] M. Oudi, K. Sanchooli Tazeh, N. Hazeri, M. Fatahpour, R. Ahmadi, *J. Chin. Chem. Soc.* **2019**, *66*(12), 1721.

[37] M. Dabiri, M. Bahramnejad, M. Baghbanzadeh, *Tetrahedron* **2009**, *65*(45), 9443.

[38] L. Moradi, Z. Ataei, Z. Zahraei, *J. Iran. Chem. Soc* **2019**, *16*(6), 1273.

[39] N. Mohammadian, B. Akhlaghinia, *Res. Chem. Intermed.* **2019**, *45*(10), 4737.

[40] K. Hemmat, M. A. Nasseri, A. Allahresani, S. Ghiami, *J. Organomet. Chem.* **2019**, *903*, 120996.

[41] B. Zamani-Ranjbar-Garmroodi, M. A. Nasseri, A. Allahresani, K. Hemmat, *Res. Chem. Intermed.* **2019**, *45*, 5665.

## SUPPORTING INFORMATION

Additional supporting information may be found online in the Supporting Information section at the end of this article.

**How to cite this article:** Faroughi Niya H, Hazeri N, Fatahpour M. Synthesis, characterization, and application of $CoFe_2O_4$@amino-2-naphthol-4-sulfonic acid as a novel and reusable catalyst for the synthesis of spirochromene derivatives. *Appl Organomet Chem*. 2020;e6119. https://doi.org/10.1002/aoc.6119